

# MAKING SENSE OF SUNSPOT DECAY

## *I: Parabolic Decay Law and Gnevyshev–Waldmeier Relation*

K. PETROVAY

*Instituto de Astrofísica de Canarias, La Laguna, Tenerife, E-38200 Spain*

L. VAN DRIEL-GESZTELYI

*Observatoire de Paris, DASOP, F-92195 Meudon Cedex, France, and  
Konkoly Observatory, Budapest, Pf. 67, H-1525, Hungary*

[*Solar Physics* **166**, 249-266 (1997)]

**Abstract.** In a statistical study of the decay of individual sunspots based on DPR data we find that the mean instantaneous area decay rate is related to the spot radius  $r$  and the maximal radius  $r_0$  as  $D = C_D r/r_0$ ,  $C_D = 32.0 \pm 0.26$  MSH/day. This implies that sunspots on the mean follow a parabolic decay law; the traditional linear decay law is excluded by the data. The validity of the Gnevyshev–Waldmeier relationship between the maximal area  $A_0$  and lifetime  $T$  of a spot group,  $A_0/T \simeq 10$  MSH/day, is also demonstrated for individual sunspots. No evidence is found for a supposed supergranular “quantization” of sunspot areas. Our results strongly support the recent turbulent erosion model of sunspot decay while all other models are excluded.

**Abbreviations:** CM – central meridian; DPR – Debrecen Photoheliographic Results; GPR – Greenwich Photoheliographic Results; MSH – millionth solar hemisphere; MSHER – MSH equivalent radius

## 1. Introduction

It has been known since the era of the first telescopic observations that sunspots disappear from the face of the Sun on a timescale of days/weeks by a gradual shrinking (sometimes punctuated by fragmentation events). During this process of decay the boundary of the spot remains well defined and its temperature deficit does not change too much (nor does its magnetic field strength vary by more than about 20%, cf. Collados *et al.*, 1994; Steinegger *et al.*, 1996). The extremely large individual variations among spots however did not make it possible to find quantitative regularities in the decay until the availability of sufficiently large and precise observational databases (GPR, Pulkovo, Mt. Wilson). These studies began in earnest towards the middle of this century, and by about 1970, two simple statistical relationships had become rather widely accepted among solar physicists:

- The rule of the proportionality of the maximal area  $A_0$  of a sunspot group to its lifetime  $T$  (first plotted by Gnevyshev, 1938, and formulated by Waldmeier, 1955):

$$A_0 = \overline{D}_{\text{GW}} T \quad \overline{D}_{\text{GW}} \sim 10 \text{ MSH/day.} \quad (1)$$

- The alleged linear time-dependence of the area during the phase of decay:

$$A = A_0 - \overline{D}(t - t_0). \quad (2)$$

This formula was originally proposed by Bumba (1963) for recurrent sunspot groups, while for the majority of non-recurrent groups a concave decay curve was found to be a better fit. However, for a variety of reasons including bad sampling intervals and large scatter, significant departures of the decay curve from linear were difficult to find and even more difficult to describe quantitatively. Thus, the linear decay law had become widely accepted as the simplest approximation to the decay curves (Ringnes, 1964a, 1964b; Robinson and Boice, 1982).

More recently, doubt has been cast on the validity of the linear decay law. Moreno-Insertis and Vázquez (1988) and Martínez Pillet, Moreno-Insertis, and Vázquez (1993) pointed out that the statistical evidence for a parabolic decay law

$$A = A_0 - 2\sqrt{\pi A_0}w(t - t_0) + \pi w^2(t - t_0)^2 \quad (3)$$

is somewhat stronger than for a linear decay. Such a decay law would follow from a slow inwards motion of the spot boundary with a constant velocity  $w$ . However, a definite conclusion about the significance of that result could not be drawn. The correct form of the sunspot decay law has thus remained undetermined.

Note also that the Gnevyshev–Waldmeier relation (1) was derived for sunspot *groups*, and its validity for individual spots has not been demonstrated.

Another open question is that of the existence of preferred length/area scales corresponding to higher stability of the spots (i.e. to lower decay rates). Such a “quantized” character of the distribution of sunspot areas (possibly caused by interaction with supergranulation) has been proposed by several authors (Ikhsanov, 1967; Dmitrieva, Kopecký, and Kuklin, 1968; Bumba, Ranzinger, and Suda, 1973). The statistical significance of those findings however remains dubious.

In this paper we present the results of a statistical investigation aimed at resolving these fundamental open questions related to sunspot decay. (Preliminary results of this study have been published elsewhere: Petrovay and van Driel-Gesztelyi, 1997.) Our investigation yields definitive answers to the issues mentioned above. This has been made possible by our use of the Debrecen Photoheliographic Results: this recently published database is the only data set of statistically significant size to contain parameters for individual sunspots with day-to-day identification, measured and reduced by very high standards of precision.

The available theories and models of sunspot decay served as our guide during the analysis by concentrating our attention to those correlations for which different models had different predictions. We are thus also able to exclude some of those models, leaving a single one compatible with the observational constraints. The models and their predictions are outlined in Section 2. In Section 3 we discuss our selection and handling of data in detail, while Sections 4 and 5 present the results. Section 6 concludes the paper.

## 2. Models

The first quantitative model for sunspot decay was proposed by Gokhale and Zwaan (1972). To explain the observed sharp boundary of spots they assumed that the magnetic flux tube is surrounded by a current sheet, i.e. that moving outwards from the spot center, the magnetic flux density drops to zero in a very narrow radius range. They further assumed that turbulence is fully inhibited by the strong magnetic field in and inside the current sheet, so that the decay of the spot is only due to pure Ohmic dissipation in the current sheet. They pointed out that a linear decay law implies that the thickness of the current sheet must be a constant fraction of the radius, i.e. the spot remains *self-similar* during the decay. In order to produce an ever thinner current sheet, however, they needed to postulate *ad hoc* the existence of a radial inflow towards the tube, for which no observational indication existed. For this reason, their model never became so widely accepted as the turbulent diffusion model.

The latter model, proposed independently by Meyer *et al.* (1974) and by Krause and Rüdiger (1975), assumes that the decay of the spot is caused by turbulent diffusion throughout the whole cross-section of the tube, with a magnetically reduced but otherwise constant diffusivity. It was found that defining the boundary of the spot at some arbitrary fixed value of the flux density, such a diffusion naturally results in a linear decay law, and the Gnevyshev–Waldmeier relation is also returned. The diffusivity was essentially treated as an adjustable parameter. The tubes in this model had no sharp boundary, being gradually “washed away” by diffusion, and the central flux density showed a gradual decrease instead of remaining more or less constant until the full decay of the spot. The model is also problematic from a theoretical point of view, as a constant magnetically reduced diffusivity is hardly compatible with a magnetic field that must obviously be lower outside the tube. Despite these obvious shortcomings, its prediction of the two (alleged) linear laws of sunspot decay made this model the most accepted theoretical explanation of the decay for two decades.

The studies of Moreno-Insertis and Vázquez (1988) and Martínez Pillet, Moreno-Insertis, and Vázquez (1993) questioned the validity of the linear decay law, reviving the old suggestion (Simon and Leighton, 1964) that the decay of a spot may proceed by the eroding action of *external* turbulence that “gnaws” off bits and pieces of the flux tube. It was time to reconsider the quantitative decay models. The recent *turbulent erosion model* (Petrovay and Moreno-Insertis, 1997) is formally a generalization of the turbulent diffusion model allowing a variable diffusivity explicitly depending on the magnetic field. The solutions of the nonlinear diffusion equation in cylindrical geometry

$$\frac{\partial}{\partial t} (\tilde{r}B) = \frac{\partial}{\partial \tilde{r}} \left[ \tilde{r} \nu(B) \frac{\partial B}{\partial \tilde{r}} \right] \quad (4)$$

were investigated by numerical and analytical methods. Here,  $B$  is the magnetic flux density,  $\tilde{r}$  is the radial coordinate, and  $\nu$  is the turbulent magnetic diffusivity. For the dependence of the diffusivity on the magnetic field they considered a simple function satisfying the basic physical requirements:

$$\nu(B) = \frac{\nu_0}{1 + |B/B_e|^{\alpha_\nu}}. \quad (5)$$

Here  $\alpha_\nu$  is a parameter quantifying the steepness of the diffusivity cutoff near  $B_e$ , the latter being the field strength where the diffusivity is reduced by 50%. Physically, one expects  $B_e \sim B_{\text{eq}}$ , the kinetic energy density of photospheric turbulence. The solutions of Equation (4) were found to be qualitatively similar to the case with constant diffusivity as long as the inhibition of turbulence was weak (i.e. for low values of  $\alpha_\nu$  and/or  $B_0/B_e$ ,  $B_0$  being the central field strength of the initial field profile). For strong inhibition of turbulence however a new class of solutions sets in: a *current sheet* is spontaneously formed around the tube, moving inwards with a constant speed  $w$ , while the field strength inside the current sheet remains practically unchanged during the decay until the arrival of the current sheet. This leads to a parabolic decay of the cross section of the tube.

An important and attractive feature of the erosion model is that the velocity  $w$  of the current sheet becomes asymptotically independent of  $\alpha_\nu$ , i.e. for  $\alpha_\nu \rightarrow \infty$  it goes to the finite limit

$$w \simeq 2^{-1/3} \frac{B_e}{B_0 - B_e} \frac{\nu_0}{r_0}, \quad (6)$$

where  $r_0$  is the maximal radius of the spot. Thus, the lifetime of the spot remains finite even for infinitely effective inhibition of the turbulence inside the tube.

Using Equation (6) and assuming that the unperturbed value of the diffusivity outside the tube is  $\nu_0 = 1000 \text{ km}^2/\text{s}$ , i.e. the granular value,

Table I  
Predictions of different sunspot decay models.

|               | Self-similar<br>sunspot   | Turbulent<br>diffusion                                |
|---------------|---------------------------|---|
| Decay law     | $D = \text{const.}$       | $D = \text{const}$                                    |
| Lifetime      | $T \propto A_0$           | $T \propto A_0$                                       |
| $B_0(t)$      | constant                  | gradual decrease                                      |
| Spot boundary | sharp                     | diffuse   |
| Reference     | Gokhale &<br>Zwaan (1972) | Meyer <i>et al.</i> (1974)<br>Krause & Rüdiger (1975) |

|               | Turbulent<br>erosion                 | Universal<br>parabolic                  |
|---------------|--------------------------------------|---|
| Decay law     | $D \propto r/r_0$                    | $D \propto r$                           |
| Lifetime      | $T \propto A_0$                      | $T \propto \sqrt{A_0}$                  |
| $B_0(t)$      | constant                             | constant                                |
| Spot boundary | sharp                                | sharp                                   |
| Reference     | Petrovay &<br>Moreno-Insertis (1997) | Martínez Pillet<br><i>et al.</i> (1993) |

$B_0 = 3000$  G and  $B_e = 400$  G, one finds that the Gnevyshev–Waldmeier rule is returned:

$$r_0/w \simeq 2^{1/3} \frac{B_0 - B_e}{B_e} \frac{r_0^2}{\nu_0} = A_0/\bar{D} \quad \bar{D} \simeq 10. \quad (7)$$

For the instantaneous decay rate  $D = \dot{A}$  in turn we have the prediction

$$D \simeq \left( 2^{2/3} \pi \nu_0 \frac{B_e}{B_0 - B_e} \right) \frac{r}{r_0} = C_D \frac{r}{r_0} \quad C_D \simeq 22. \quad (8)$$

The predictions of different published decay models are summarized in Table I. The “universal parabolic” model in the table is identical to the turbulent erosion model except that the current sheet velocity  $w$  is assumed to be a universal constant instead of depending on the maximal spot radius as in Equation (6). This “model” has no theoretical foundation, and it was only tentatively suggested by Martínez Pillet, Moreno-Insertis, and Vázquez (1993) to forge a link between the lognormal distributions of decay rates and spot areas.

### 3. Data

#### 3.1. SELECTION

DPR data for the years 1977 and 78 (Dezső, Gerlei, and Kovács, 1987; Dezső, Gerlei, and Kovács, 1997) were used, selecting only spots with maximal areas exceeding 10 MSH and measurements made within  $\pm 72^\circ$  of the central meridian. In the following, this part of the solar surface will be referred to as “the visible hemisphere”. For the present study only total (umbra+penumbra) areas are used. Altogether, our data set consisted of 3990 area measurements for 476 different spots.

The nominal error of measurements in the DPR is less than 1 MSH, implying a “worst case” visibility function (Kopecký, Kuklin, and Starkova, 1985)  $\sec^2 \lambda$  where  $\lambda$  is the angular distance from the center of the disk. Variable exposure times and seeing conditions, aggravated by the geometric foreshortening correction factors for higher  $\lambda$ 's however lead to a larger random error in the area measurements. The Introduction of the DPR (Dezső, Gerlei, and Kovács, 1987) quotes error values of typically 5%, reaching 20% for the smallest spots in the sample. In spite of the great precision and care the DPR was compiled with, there is also a small chance for errors in the spot identification, especially in complicated, quickly changing sunspot groups. These errors are small compared to the random physical scatter present in the data, and being random, they cannot contribute to the physical correlations we find in Sections 4 and 5.

A *systematic error* is also involved owing to the physical foreshortening (Archenhold, 1940). While this error can be quite significant for small spots close to the  $\pm 72^\circ$  CM distance limits, it will not exert a great influence on a sample as a whole unless the spots of that sample have a strong tendency to be situated close to the limits. Such a tendency is known to be present in at least one case. The first observation of a spot on the “visible hemisphere” is considered as its *birth* if the spot was not seen at the previous observing time (typically, the previous day). The *death* of a spot is defined in an analogous manner. While the distribution of birth and death sites has a well-known East–West asymmetry, peaking near the limbs, a straightforward estimate following the method of Kopecký, Kuklin, and Starkova (1985) shows that with the visibility function quoted above the effect is small, and birth and death sites in our sample are distributed nearly uniformly, i.e. the systematic error is small.

One should also be aware that some steps in the compilation of the data set lead to *selection effects*. An obvious effect is that the DPR database only includes spots for which at least 2 observations exist. Taking into account that observations are typically separated by 1-day (and occasionally 2 to 4-day) intervals, this implies that our sample is not complete below lifetimes

of about 5 days. In what follows, this effect will be referred to as the *short lifetime selection effect*.

Another effect is the *visibility reduction of lifetime* (Kopecký, Kuklin, and Starkova, 1985) which will cause a systematic error downwards in determined spot lifetimes. The error is maximal for lifetimes of 8–10 days, but with the visibility function at hand it altogether remains small.

### 3.2. DEFINITIONS

Let us assume that a given spot was observed at times  $t_1, \dots, t_N$ , the corresponding area values being  $A_1, \dots, A_N$ . If  $t_1$  and  $t_N$  correspond to the actual birth and death of the spot, as defined in Section 3.1 above, then the *lifetime* of the spot is given by

$$T \stackrel{\text{def}}{=} t_N - t_1 + 1^{\text{d}} \quad (9)$$

For each measured area value the *equivalent radius*  $r_i$  of the circle having the same area is computed. In this paper, equivalent radii will be expressed in MSHER units: a spot of radius 1 MSHER has an area of 1 MSH, so that in these units  $A_i = r_i^2$  (1 MSH = 3044 km<sup>2</sup>, 1 MSHER = 984 km.) Time will be measured in days. The spot is regarded to be in a decay phase at time  $t_i$  if  $r_{i-1} \geq r_i > r_{i+1}$  holds (or if  $r_{N-1} \geq r_N$ , in the case of the last observation). The “instantaneous” decay rate of the spot is then given by  $D_i = 2\pi r_i w_i$  where  $w$  is the velocity of the spot boundary, calculated from

$$w_i = w_i^{(0)} + 2 \frac{(w_i^{(1)} - w_i^{(0)})(t_i - t_{i-1})}{(t_{i+1} - t_{i-1})^2} \quad (10)$$

$$w_i^{(j)} = \frac{r_{i-1+j} - r_{i+j}}{t_{i+j} - t_{i-1+j}} \quad (11)$$

In the case of the last observation,  $w$  is calculated for a time  $t_{N'} = (t_{N-1} + t_N)/2$  from

$$w_{N'} = \frac{r_{N-1} - r_N}{t_N - t_{N-1}}. \quad (12)$$

We note that the above formulae imply the assumption  $w = \text{const.}$  between observations, i.e. a parabolic decay law. In order to ensure that our results are not distorted by such a tacit assumption, we repeated all statistical studies by using an alternative definition for  $D$ , based on a linear decay law. The results of Sections 4 and 5 were not significantly influenced by this choice. As those results exclude the linear decay law, here we use the above formulae in all calculations.

Similar care must be exercised with the definition of the maximal spot area  $A_0$ , corresponding to an equivalent radius  $r_0$ , at time  $t_0$ . Many complex

spots show several local maxima (and consequently several decay phases) in their  $A(t)$  curves, so the definition of a single maximum is not unique. For the results presented in this paper the maximum was defined as the *absolute* maximum *preceding* the given observation of the spot:

$$A_{0,i} = \text{Max} \{A_j\}_{j=1,\dots,i} \quad A_0 \equiv A_{0,N}. \quad (13)$$

Again, using alternative definitions for the maximum, the results were not significantly influenced (although using the preceding local maximum instead of the absolute maximum made most correlations somewhat worse).

Another problem related to maximum determination is that owing to the rotation of the Sun, in many cases we cannot follow the complete evolution of the spot. In these cases we cannot be sure if the absolute maximum we determined is *really* the absolute maximal area of the spot during its prior evolution. In order to deal with this problem, the sample was divided into subsamples of different “reliability” (e.g. spots born and died on the visible hemisphere etc.). While using a more carefully selected sample does reduce the scatter in statistical relationships, it may also reduce the significance of the result owing to the lower number of data. Again, most of the studies presented in Sections 4 and 5 were performed on different subsamples. The results presented here use subsamples chosen to minimize the scatter while being still large enough to be statistically significant.

### 3.3. BIAS CORRECTIONS

The explicit selection effects mentioned in Section 3.1 above originate from conscious decisions during the compilation of the data set. Our sample is however also affected by *implicit selection effects* or *biases*. A bias here means that the distribution of some variable  $y$  in our data set will differ from its actual distribution among sunspots because the *expected number of observations* for one spot depends on  $y$ . Let  $\hat{P}(y; \mathbf{x})$  denote the observed distribution of  $y$  in some subset of our data homogeneous in the variable(s) symbolically denoted here by  $\mathbf{x}$ . If the real distribution (i.e. the “spot distribution” as opposed to the “data distribution”) is denoted by  $P(y; \mathbf{x})$  and the expected number of data for one spot by  $p(y; \mathbf{x})$  then clearly

$$P(y; \mathbf{x}) = F(y; \mathbf{x}) \hat{P}(y; \mathbf{x}) \quad (14)$$

where  $F \propto 1/p$ , with some arbitrary normalization. It is convenient to choose the normalization so that in our discrete sample of  $N$  data,  $\sum_{i=1}^N F_i = N$ . Formulae for  $p$  viz. for the correction factor  $F$  for cases of practical importance will be given below.



Often we are only interested in the mean and the standard deviation of  $P$ . These and their r.m.s. errors are given by

$$\bar{y} = \langle yP \rangle = \frac{1}{N} \sum_{i=1}^N y_i F_i \quad (15)$$

$$\sigma^2 = \langle (y - \bar{y})^2 P \rangle = \frac{1}{(N-1)} \sum_{i=1}^N (y_i - \bar{y})^2 F_i \quad (16)$$

$$\sigma_y^2 = \sigma^2 \sum_{i=1}^N \left( \frac{\partial \bar{y}}{\partial y_i} \right)^2 = \frac{\sigma^2}{N^2} \sum_{i=1}^N \left( F_i + y_i \frac{\partial F_i}{\partial y_i} \right)^2 \quad (17)$$

$$\begin{aligned} \sigma_\sigma^2 &= \sigma^2 \sum_{i=1}^N \left( \frac{\partial \sigma}{\partial y_i} \right)^2 = \\ &= \frac{1}{4(N-1)^2} \sum_{i=1}^N \left[ 2(y_i - \bar{y})F_i + (y_i - \bar{y})^2 \frac{\partial F_i}{\partial y_i} \right]^2 \end{aligned} \quad (18)$$

If one wishes to make a least-squares fit  $y = y_0(\mathbf{x})$  to the data, the simplest way to do this for a biased sample is to bin the data in  $\mathbf{x}$  using bins small enough that  $y_0$  may be securely assumed to be nearly constant within each bin. Then  $\bar{y}$  is calculated for each bin from Equation (15), and the fit is performed on these bin averages, weighting each value by the inverse of its  $\sigma_y^2$ , as given by Equation (17).

### 3.3.1. $y = f(T)$ : *Gnevyshev–Ringnes correction*

The lifetime of a spot can obviously only be determined if both its birth and death occur in the visible hemisphere, so only such spots will enter our data set. The probability  $p$  of this being so (i.e. the expected number of data for one spot) however depends on  $T$  according to a formula first given by Gnevyshev (1938) and later corrected by Ringnes (1964c). For our purposes this can be written as

$$p = \begin{cases} 0 & \text{if } |\alpha| \geq 2\theta_0 \\ \frac{2\theta_0 - |\alpha|}{360^\circ} & \text{if } |\alpha| < 2\theta_0 \end{cases} \quad (19)$$

$$\alpha \stackrel{\text{def}}{=} [180^\circ - (\Omega T + 180^\circ) \bmod 360^\circ] \quad (20)$$

Here,  $\theta_0 = 72^\circ$  is the CM distance limit and  $\Omega = 360^\circ / P_{\text{syn}}$ ,  $P_{\text{syn}}$  being the synodic rotation period of the given spot. For simplicity, here we use the value  $P_{\text{syn}} = 28^{\text{d}}$  for all spots. (In 1977/78 sunspots were situated at high latitudes.)

The correction factor  $F$  is the normalized inverse of Equation (19), independently of the form of the function  $f(T)$ . Its derivative  $F'(y)$ , entering Equations (17) and (18), will obviously depend on that form, though. In Section 5 below we will deal with the distribution of  $y = \log T$ : in that case  $F'(\log T) = \ln 10 TF'(T)$ .

### 3.3.2. $y = f[D; g(A, A_0)]$ : correction for the decay law

Let us first restrict our interest to the case  $g(A, A_0) = A$ . In this case our study of the distribution of  $y$  is limited to spots in the area interval  $[A, A + dA]$ . A spot with a decay rate  $D$  will spend a time  $dA/D$  in this interval, so if our observations are made with  $1^d$  intervals, the expected number of observations for one spot in that interval (in our units of measurement) is clearly  $p = dA/D$ . In the more general case

$$p = \frac{dA}{dg} \frac{dg}{D}. \quad (21)$$

It is apparent that  $p$  (and  $F$ ) here depend on the form of the  $g(A, A_0)$  function. This is in contrast to the Gnevyshev–Ringnes correction where the observation probability of a spot of lifetime  $T$  was independent of any other spot parameter than  $T$ . For the two cases investigated in Section 4 below the correction factor takes the form

$$F = \begin{cases} F_0 \frac{D}{A_0 g} & \text{if } g = (A/A_0)^{1/2} \\ F_0 \frac{D}{g} & \text{if } g = A^{1/2} \end{cases} \quad (22)$$

$F_0$  being a normalization factor.  $F$  is again independent of the form of  $f(D)$  while its derivative for  $y = \log D$  is  $F' = \ln 10 F$ .

### 3.3.3. Limitations of the bias correction

Assume that all our measured  $y_i$  data fall within an interval  $J$ . If  $p \gg 1/N$  in the neighbouring intervals of similar size then we can be reasonably sure that the lack of data points outside the above range is not an artefact caused by the bias. (This is the case with our studies in Section 4.) If however the range of strong bias  $p \lesssim 1/N$  overlaps  $J$  or is immediately adjacent to it, we should suspect that the lack of data in the strong bias range is an artefact. In this case, no proper correction is possible. The values derived for the mean and standard deviation, however, may still be acceptable [albeit with the large error bar given by Equation (17)] if data points are present both above and below the strong bias range, thereby offering the possibility of an interpolation. This is the case we will encounter in Section 5.

Beside the implicit selection effects dealt with above, there is a variety of subtle biases affecting certain distributions, the corrections of which is not

always straightforward or worth the effort. We will meet two such examples in the following section. Unfortunately, neither these more involved selection effects nor others discussed in Sections 3.1 and 3.3 were properly taken into account in much of the earlier work on the subject.

#### 4. Decay law

##### 4.1. $D$ vs. $r/r_0$

Guided by the prediction of the turbulent erosion model, Equation (8), in Figure 1 we plot the instantaneous decay rates  $D$  against the relative radius  $r/r_0$  [in the sense of  $r_i/r_{0,i}$ , cf. Equation(13)]. In this plot we show measurements for those spots which died on the visible hemisphere (888 data points, 170 of these for recurrent spots). The results for the complete sample are however very similar. As sunspot decay rates are lognormally distributed (Martínez Pillet, Moreno-Insertis, and Vázquez, 1993; see also the following paper in this series), for the application of Gaussian-based statistical methods (least squares etc.)  $D$  should be plotted on a logarithmic scale.

It is apparent that the formula (8) is indeed a reasonable representation of the data. Binning the data in  $r/r_0$  and correcting the bias described in Section 3.3.2 we find that a constant  $D$  (i.e. a linear decay law) can be excluded at a very high confidence level ( $Q = \Gamma[(N - 1)/2, \chi^2/2] < 10^{-5}$ ). In contrast, a linear fit of the form  $D = C_D r/r_0$  (i.e. a parabolic decay law, the best fit being  $C_D = 32.0 \pm 0.26$ ) yields an excellent agreement ( $Q = 0.68$ ). The difference in the coefficient compared to Equation (8) can be easily accommodated taking into account the uncertainty of the value of  $\nu_0$ , the strong height-dependence of  $B_e$ , and the fact that our formula (8) was based on the infinite  $\alpha_\nu$  limit (6), so the actual value of  $w$  may be somewhat higher.

The question arises, how is it possible that this obvious nonlinearity of the decay had not been noticed earlier? While our use of the DPR with its high precision individual sunspot area data may be a factor in a more conclusive result, the study of Moreno-Insertis and Vázquez (1988) shows that with proper methods of analysis a nonlinearity can also be detected in the GPR data. We should therefore suspect that the choice of the technique of analysis is a crucial factor in this respect. Sunspot decay curves are usually characterized by bad sampling intervals: for short-lived spots one often only has 2–3 measurements in the decay phase, while for recurrent spots a large number of measurements are grouped together in the vicinity of 2–3 points of the decay curve. The true endpoint of the decay curve is thus ill determined and the method of producing “typical” decay curves by

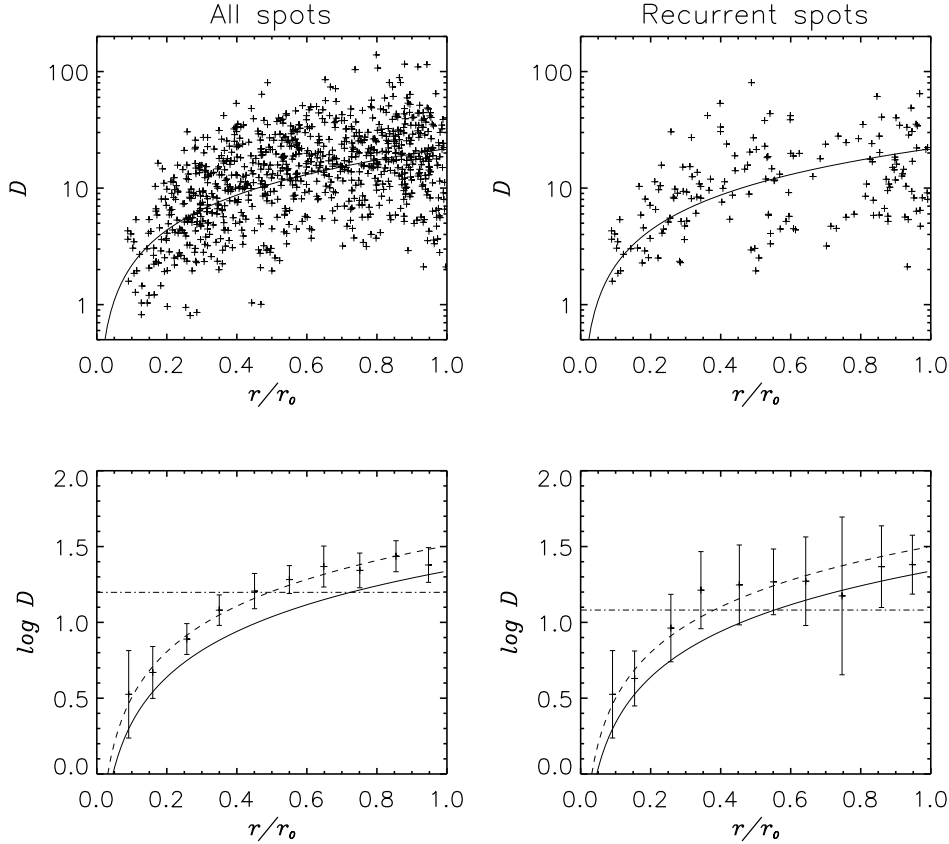


*Figure 1.* Decay rates plotted against relative radius for the original (top) and binned (bottom) data. Data for spots which died on the visible hemisphere are shown. Solid line: Equation (8). Dashed line: linear least-squares fit. (Here and in all other figures,  $2\sigma$  error bars for the mean are shown.)

time-shifting individual curves to a common endpoint (e.g. Ringnes, 1964a, 1964b) implies rather large errors. These errors are further aggravated by the fact that the lifetime–maximal area correlation (cf. Section 5) involves a large scatter, thus spots with greatly different  $r_0$  values will enter the sample, leading to different decay rates at the same time. The resulting large scatter in  $D$  will tend to smear out any nonlinearity. This is borne out in Figure 2 where the parabolic decay curve is directly seen in the subsample with  $A_0$  in a narrow range (bottom left panel), while the picture is much more confuse if no such selection is performed (top left panel). (Note that some non-linearity is still visible even in this latter panel. This may be due to our time-shifting the curves to a common maximum instead of a common endpoint, as usual.) The selection of an  $A_0$ -limited subsample however

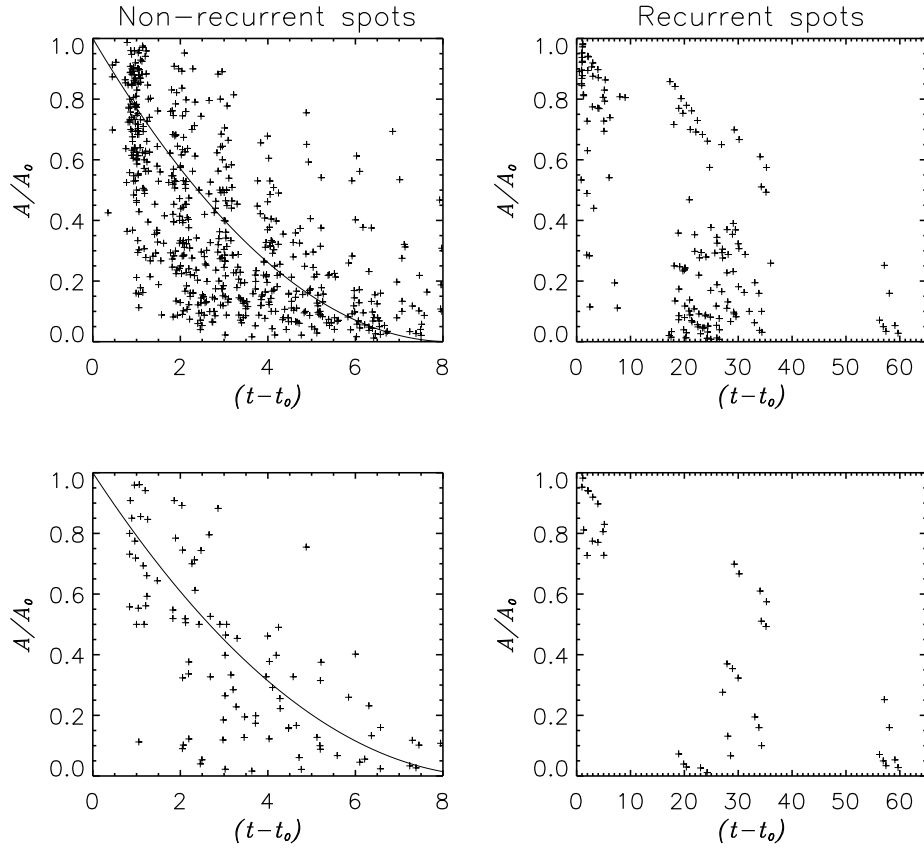


Figure 2. Relative area vs. time plots. *Top*: all spots; *bottom*: spots with maximal areas in a restricted range (90–110 for non-recurrents, 250–350 for recurrents). Solid line: Equation (3) with  $A_0 = 90$  and  $w$  from Eqs. (6) and (8)

greatly reduces the sample size making it difficult to establish the nonlinearity at a high confidence level for all but the most frequent  $A_0$  values. Thus, the  $D-r/r_0$  plot (Figure 1) is much more useful for the study of the decay law.

The study of Bumba (1963) resulted in a nonlinear decay law for the majority of non-recurrent spots while a linear decay law was found to describe the recurrent spots. To check the reality of such a distinction, in the right-hand panels of Figure 1 we present the  $D-r/r_0$  plot for recurrent spots only. Essentially the same results are found as for the complete sample. This is so despite the fact that this plot is distorted by an uncorrected bias: the apparent local minimum near  $r/r_0 \simeq 0.7$  is caused by the fact that between the first and second disk passages, higher- $D$  spots shrink more —so the corresponding gap in  $r/r_0$  will be wider in the upper part of the diagram.

Bumba’s finding could be due to the fact that the  $A_0$  values of recurrent spots are scattered within very wide limits. This, together with the bad sampling intervals, leads to a very confuse area–time plot (right hand panels in Figure 2), for which a linear fit is as good as anything else.

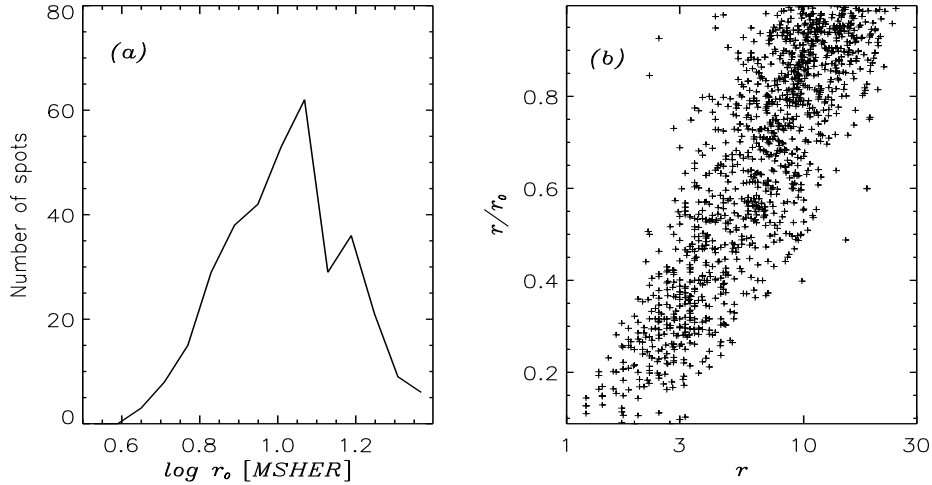


Figure 3. Histogram of maximal radii (a) and  $r$  vs.  $r/r_0$  plot (b) for all spots in our data set.

#### 4.2. $D$ vs. $r$

Having excluded the linear decay law and shown that  $D \propto r/r_0$  is compatible with the data, we still need to check the validity of the prediction of the fourth model in Table I, i.e. the “universal parabolic” decay law  $D \propto r$ . This is necessary because in our data there is a good, nearly linear correlation between  $r$  and  $r/r_0$ , caused by the rather sharp peak in the distribution of  $r_0$  values, as illustrated in Figure 3. (Note that this histogram is contaminated by several selection effects, but this is irrelevant for our present purpose.) The suspicion arises that the correlation between  $D$  and  $r/r_0$  found above might be just a reflection of a more basic relationship between  $D$  and  $r$ .

The distribution of the data points from the full sample (1234 points) on the  $r$ – $D$  plane is shown in Figure 4. It turns out that a fit of the form  $D \propto r$ , corresponding to the universal parabolic model, is incompatible with the data ( $Q < 10^{-5}$ ), as is a constant decay rate.

The actual distribution of the data finds its explanation in Figure 4d. For  $r \gtrsim 7$ , there is a nearly one-to-one correspondence between  $r$  and  $r_0$ , i.e. most of these measurements refer to spots close to their maximal radii. This is a consequence of the rather fast decrease of the  $r_0$  distribution curve,

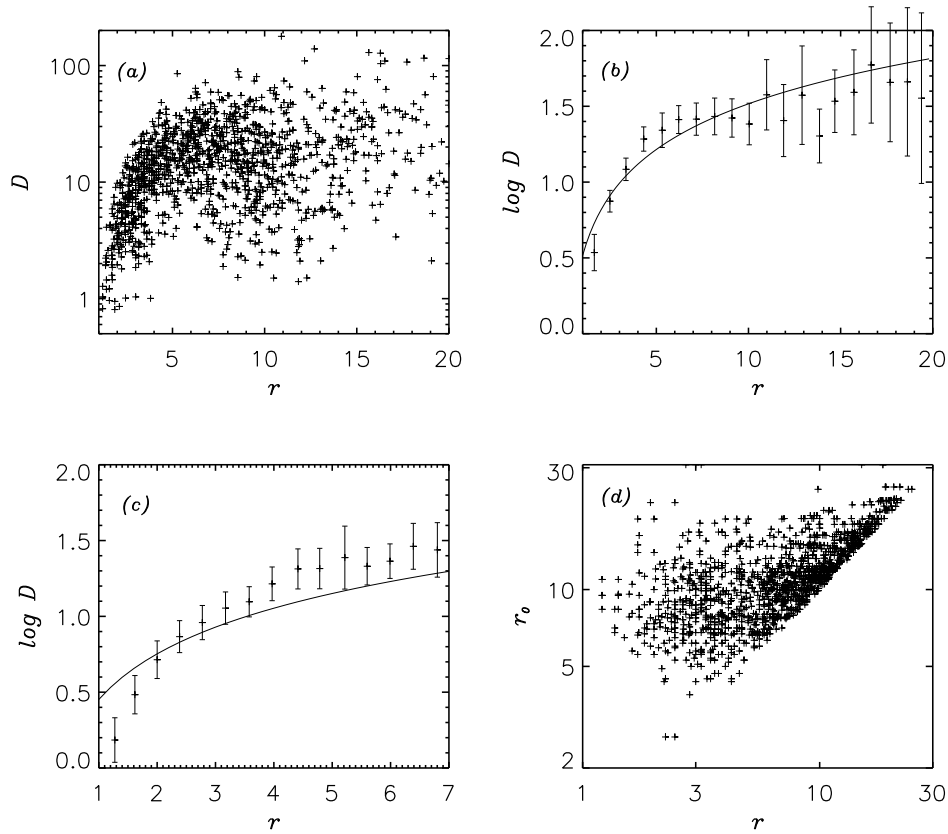


Figure 4.  $D$ - $r$  plot for the original (a) and binned (b) data. (c): low  $r$  part with higher resolution; (d):  $r$  vs.  $r_0$  plot. All decay rate measurements are shown. Solid line: linear least-squares fit.

Figure 3a, in this regime. According to Equation (8), the decay rate is then constant: indeed, for  $r \gtrsim 7$  the  $D$ - $r$  plot is compatible with  $D = \text{constant}$ . The sharp peak in the histogram of  $r_0$  near 10 also implies that for lower values of  $r$  most of the measurements are for spots with  $r_0 \simeq 10 = \text{const}$ . Thus, as it follows from Equation (8), in the range  $r = 3$ -7 the  $D$ - $r$  distribution is reasonably well fit by the linear relation  $D \propto r$ .

In the range  $r \lesssim 3$  the distribution again seems to depart from the linear law, this time being steeper. This is the consequence of a subtle bias: the 1-day sampling interval is relatively “coarser” for small (and thus short-lived, cf. Section 5) spots which are thus less likely to be “caught” in the latest stages of their decay. Consequently, the mean value of  $r_0$  begins to increase again with decreasing  $r$  in this regime, Figure 4d.

The fact that the  $D$ - $r$  relation for  $r > 7$  is compatible with a constant decay rate implies that we have no significant evidence for the existence of a supergranular area “quantum” where spots are supposed to be more stable, decaying slower. An independent test of this was also performed by taking the power spectrum of the histogram of  $r$  (not shown here): again, no significant peaks were found. The area histogram published by Howard (1996) leads to similar conclusions. While it cannot be excluded that using a much larger database, such an effect may be discovered in the future (note the slight local minimum in the  $D$ - $r$  plot near  $r \simeq 14$ ), none of the papers that claimed to have found such a quantization was in fact based on a database significantly more extensive than ours in the given area range ( $\gtrsim 80$  MSH). Some of these works used data for “regular” spots only, the selection criteria however were rather subjective. Facing this state of the matter, we are forced to conclude that no compelling evidence exists for the supposed phenomenon of quantized sunspot areas.

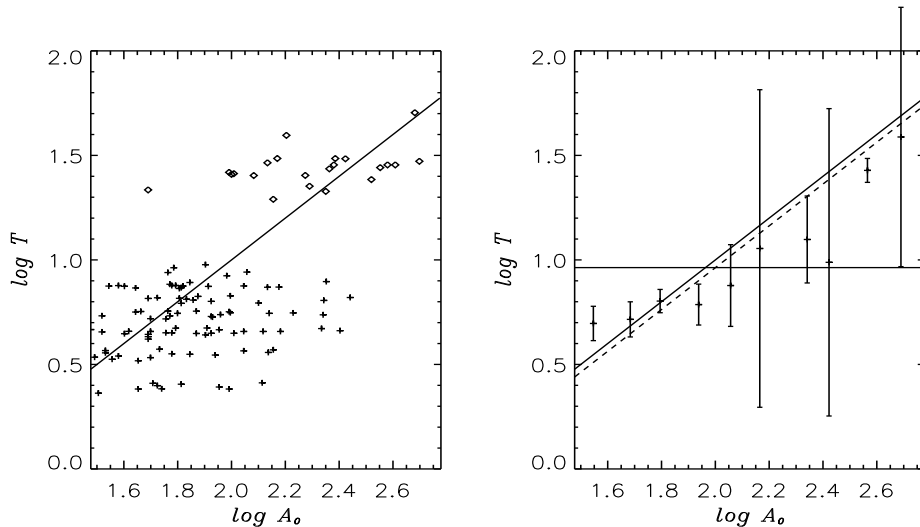


Figure 5. Area-lifetime relation for all spots with determined lifetimes in the 1977/78 DPR data. +: non-recurrent spots;  $\diamond$ : recurrent spots. Solid line: Gnevyshev–Waldmeier relation  $A_0 = 10T$ ; dashed line: linear best fit.

## 5. Area-lifetime relation

There are 128 spots in our sample which were born on the visible hemisphere and also died there, so that their lifetime could be determined. These lifetimes are plotted against the maximal radii in Figure 5. The empty horizontal band corresponds to spots living for about half a solar rotation:



obviously, no lifetime could be determined for any of these. After binning and applying a Gnevyshev–Ringnes correction (Section 3.3.1), a linear fit  $A_0 = \overline{D}_{\text{GW}}T$  yields  $\overline{D}_{\text{GW}} = 10.89 \pm 0.18$ , in excellent agreement with Equation (1). The validity of the Gnevyshev–Waldmeier rule is thus also proven for individual sunspots.

Note that from Equation (8) with the value  $C_D = 32$  derived in the previous section a mean decay rate of  $\overline{D} = 16$  would follow. This does not contradict to the value of  $\overline{D}_{\text{GW}}$  derived here, as here we are dealing with the ratio of the maximal area to the *full* lifetime of the spot which is typically larger than the decay time by about 40 % (Vitinsky, Kopecký, and Kuklin, 1986).

The data obviously show a rather large scatter around the linear law, and the presence of exclusion zones corresponding to lifetimes around half-integer rotations makes it even more difficult to discern the correlation, particularly for samples limited in  $T$  —e.g. Vitinsky (1956). However, a mean lifetime independent of maximal area,  $T = \text{constant}$ , is definitely excluded by the data ( $Q < 10^{-5}$ , as opposed to  $Q = 0.18$  for the linear best fit).

Some explanation may be in order as to our choice of  $A_0$  as independent variable for the fit. Using  $T$  as independent variable, as previous authors did, would clearly make it possible to avoid the use of a Gnevyshev–Ringnes correction, and it would not be sensitive to the short lifetime selection effect (Section 3.1): this latter effect leads to the slight upwards deviation of the leftmost binned data point in Figure 5, and it is the reason why the data were cut down at  $A_0 = 30$  in the figure. These advantages of a  $T$ -dependent fit are however offset by the less uniform coverage of the abscissa in that case (the low number of recurrent spots would lend a very small weight to those points in the fit) as well as by the possible strong influence of the visibility reduction of lifetime (Section 3.1) for some  $T$  values (mainly for those just below the gap). This influence may explain the suggestion by Alexander (1944) and Ringnes (1964a) that groups with a lifetime of 8 days significantly depart from the linear law. In our material we also find somewhat similar deviations near the exclusion zone, but the corresponding large error bars indicate that these are not significant.

## 6. Conclusion

In our statistical study of the decay of individual sunspots based on DPR data for the years 1977–78 we found that the instantaneous area decay rate is related to the spot radius  $r$  and the maximal radius  $r_0$  as

$$D = C_D r / r_0 \quad C_D = 32.0 \pm 0.26. \quad (23)$$

This implies that sunspots on the mean follow a parabolic decay law; the traditional linear decay law is clearly excluded by the data. A “universal” decay law of the form  $D \propto r$  is also excluded. The validity of the Gnevyshev–Waldmeier relationship between the maximal area  $A_0$  and lifetime  $T$  of a spot group

$$A_0 = \overline{D}_{\text{GW}}T \quad \overline{D}_{\text{GW}} \simeq 10 \quad (24)$$

is also demonstrated for individual sunspots. No supporting evidence is found for a supposed supergranular “quantization” of sunspot areas.

The *robustness* of these findings is worth stressing. All the subtleties of the data processing described in Section 3 will only lead to slight quantitative modifications in the correlations which are already present in the raw data.

Comparing these results with the model predictions of Table I we find that the turbulent erosion model is compatible with all the observational data while all the other models are excluded. The turbulent erosion model (Petrovay and Moreno-Insertis, 1997) assumes a strict cylindrical geometry with no dependence of the field on the coordinate along the tube. This is clearly rather far from being a good representation of real sunspots. Yet, the fact that the models are able to predict many of the essential features of sunspots, including the spontaneous formation of a current sheet around the spot and the qualitative and quantitative characteristics of the decay, suggests that the model may correctly grasp the essential underlying physics.

In this paper we have dealt with the *mean* relationships governing the decay of sunspots. In each case however a significant physical scatter is also present in the data. While this scatter is apparently “random”, it is already known that the decay properties of sunspots may correlate with their other physical characteristics. Specifically, a higher decay rate has been found to be associated with an irregular shape (Robinson and Boice, 1982), *f*-type polarity (Royal Greenwich Observatory, 1925), more bright structures in the umbra (Zwaan, 1968), or higher proper motion (Howard, 1992). The problem of random and systematic deviations from the mean laws will be treated in the following papers of this series.

### Acknowledgements

Valuable comments by Manolo Vázquez are gratefully acknowledged. This work was funded in part by the DGICYT project no. 91-0530, the DGES project no. 95-0028, and by the OTKA under grants no. F012817 and T17325.

## References

- Alexander, A. F.: 1944, *J. Brit. Astron. Assoc.* **54**, 168
- Archenhold, G. H. A.: 1940, *Monthly Notices Roy. Astron. Soc.* **100**, 645
- Bumba, V.: 1963, *Bull. Astron. Inst. Czech.* **14**, 91
- Bumba, V., Ranzinger, P., and Suda, J.: 1973, *Bull. Astron. Inst. Czech.* **24**, 22
- Collados, M., Martínez Pillet, V., Ruiz Cobo, B., del Toro Iniesta, J. C., and Vázquez, M.: 1994, *Astron. Astrophys.* **291**, 622
- Dezső, L., Gerlei, O., and Kovács, Á.: 1987, *Debrecen Photoheliographic Results for the year 1977*, Publ. Debrecen Heliophys. Obs., Heliogr. Series No. 1, Debrecen
- Dezső, L., Gerlei, O., and Kovács, Á.: 1997, *Debrecen Photoheliographic Results for the year 1978*, Publ. Debrecen Heliophys. Obs., Heliogr. Series No. 2, <ftp://fenyi.sci.klte.hu/pub/DPR/1978>
- Dmitrieva, M. G., Kopecký, M., and Kuklin, G. V.: 1968, in K. O. Kiepenheuer (ed.), *Structure and Development of Solar Active Regions*, Proc. IAU Symp. 35, Reidel, Dordrecht, p. 174
- Gnevyshev, M. N.: 1938, *Pulkovo Obs. Circ.* **24**, 37
- Gokhale, M. H. and Zwaan, C.: 1972, *Solar Phys.* **26**, 52
- Howard, R.: 1992, *Solar Phys.* **137**, 51
- Howard, R.: 1996, *Ann. Rev. Astron. Astrophys.* **34**, 75
- Ikhsanov, R. N.: 1967, *Soln. Dannye* **7**, 81
- Kopecký, M., Kuklin, G. V., and Starkova, I. P.: 1985, *Bull. Astron. Inst. Czech.* **36**, 189
- Krause, F. and Rüdiger, G.: 1975, *Solar Phys.* **42**, 107
- Martínez Pillet, V., Moreno-Insertis, F., and Vázquez, M.: 1993, *Astron. Astrophys.* **274**, 521
- Meyer, F., Schmidt, H. U., Weiss, N. O., and Wilson, P. R.: 1974, *Monthly Notices Roy. Astron. Soc.* **169**, 35
- Moreno-Insertis, F. and Vázquez, M.: 1988, *Astron. Astrophys.* **205**, 289
- Petrovay, K. and Moreno-Insertis, F.: 1997, **485**, 398
- Petrovay, K. and van Driel-Gesztelyi, L.: 1997, in B. Schmieder, J. C. del Toro Iniesta, and M. Vázquez (eds.), *Advances in the Physics of Sunspots*, Proc. 1st ASPE Euroconference, ASP Conf. Series **118**, 145
- Ringnes, T. S.: 1964a, *Astrophys. Norv.* **8**, 161
- Ringnes, T. S.: 1964b, *Astrophys. Norv.* **8**, 303
- Ringnes, T. S.: 1964c, *Astrophys. Norv.* **9**, 95
- Robinson, R. D. and Boice, D. C.: 1982, *Solar Phys.* **81**, 25
- Royal Greenwich Observatory: 1925, *Monthly Notices Roy. Astron. Soc.* **85**, 553
- Simon, G. W. and Leighton, R. B.: 1964, *Astrophys. J.* **140**, 1120
- Steinogger, M., Vázquez, M., Bonet, J. A., and Brandt, P. N.: 1996, *Astrophys. J.* **461**, 478
- Vitinsky, Y. I.: 1956, *Soln. Dannye* **6**, 145
- Vitinsky, Y. I., Kopecký, M., and Kuklin, G. V.: 1986, *Statistika Pyatnoobrazovatel'noy Deyatel'nosti Solntsa*, Nauka, Moscow
- Waldmeier, M.: 1955, *Ergebnisse und Probleme der Sonnenforschung*, 2. Aufl., Akad. Verlagsges., Leipzig
- Zwaan, C.: 1968, *Ann. Rev. Astron. Astrophys.* **6**, 135

*Address for correspondence:*

K. Petrovay  
 Instituto de Astrofísica de Canarias  
 La Laguna, Tenerife, E-38200 Spain  
 E-mail: kpetro@iac.es